

Phase equilibria in the system MgO-MgF₂-SiO₂-H₂O

CLARENCE J. DUFFY¹ AND HUGH J. GREENWOOD

Department of Geological Sciences, University of British Columbia
Vancouver, British Columbia V6T 1W5, Canada

Abstract

Unit-cell parameters as functions of mole fraction fluoro-endmember have been determined for clinohumite, chondrodite, norbergite, brucite, and sellaite. In addition, the *d* spacing for the (060) peak of talc was determined as a function of mole fraction fluoro-talc. Unit-cell parameters for the phase intermediate sellaite are

$a = 10.123$, $b = 4.6861$, $c = 3.0780\text{\AA}$ when coexisting with periclase and

$a = 10.097$, $b = 4.6812$, $c = 3.0738\text{\AA}$ when coexisting with sellaite.

From these X-ray data the compositions of coexisting phases have been determined in forty hydrothermal experiments that yielded information on eighteen different chemical equilibria. These data, combined with phase equilibrium and calorimetric data from the literature, have been treated by the method of least squares to produce a thermodynamic model for the system. The derived endmember Gibbs energies of formation from the components MgO, MgF₂, SiO₂, H₂O at 1023 K and 1 bar are in cal mol⁻¹ $\Delta G_{\text{HB}}^{\circ} = 15538$, $\Delta G_{\text{FB}}^{\circ} = 8466$, $\Delta G_{\text{HS}}^{\circ} = 44092$, $\Delta G_{\text{HN}}^{\circ} = 5333$, $\Delta G_{\text{FN}}^{\circ} = -15721$, $\Delta G_{\text{HCh}}^{\circ} = -12031$, $\Delta G_{\text{FCh}}^{\circ} = -31161$, $\Delta G_{\text{HCl}}^{\circ} = -41347$, $\Delta G_{\text{FCl}}^{\circ} = -58853$, $\Delta G_{\text{HTc}}^{\circ} = -8509$, $\Delta G_{\text{FTc}}^{\circ} = -2086$, $\Delta G_{\text{Fo}}^{\circ} = -14249$, $\Delta G_{\text{En}}^{\circ} = -7566$. Computed equilibria based upon these Gibbs energies and related excess parameters combined with entropies and heat capacities are in good agreement with data on natural assemblages.

Introduction

The system MgO-MgF₂-SiO₂-H₂O is in many respects an ideal system for experimental study. High-purity starting materials are readily available. There are no oxidation-reduction problems. Phase equilibrium and calorimetric data are abundant on important subsystems. Synthesis experiments have been carried out on the solid solution phases (Van Valkenburg, 1955, 1961; Crane and Ehlers, 1969). A basis for theoretical treatment of such systems has been given by Thompson (1967) and Muan (1967).

This study combines new experimental data on multiphase equilibria in the system with available data to form an overdetermined system of equations which describe experimentally-observed chemical equilibria. The least-squares solution of these equations is presented as a model for chemical equilibrium in the system under a wide range of conditions.

Naturally-occurring equilibria that can be represented by the model have received little attention in the literature. This is more probably due to the difficulty of obtaining fluorine analyses than to the scarcity of suitable bulk compositions. What information does exist agrees well with the model.

Symbols and units

The symbols used in this paper follow as closely as practicable the usage recommended by McGlashan (1970). Additional symbols are those in common use in the geologic literature. A list of symbols and corresponding units is given in Table 1. Table 2 lists the symbols and formula units used for the various chemical compounds encountered.

Experimental methods

Apparatus

Experiments were conducted by enclosing reagent-grade chemicals in sealed noble-metal capsules and

¹ Present address: Los Alamos Scientific Laboratory, Los Alamos, New Mexico 87545.

Table 1. Symbols and units

Table 2. Compounds considered

Quantity	Symbol	Unit	Equivalent SI Unit
Thermodynamic temperature	T	K	K
Pressure	P	bar	10^5 Pa
Molar volume of substance B	V_B	cm^3	cm^3
Molar enthalpy of substance B	H_B	cal mol^{-1}	4.184 J mol^{-1}
Molar entropy of substance B	S_B	$\text{cal mol}^{-1}\text{K}^{-1}$	$4.184 \text{ J mol}^{-1}\text{K}^{-1}$
Molar Gibbs energy of substance B	G_B	cal mol^{-1}	4.184 J mol^{-1}
Molar heat capacity of substance B at constant pressure	C_B	$\text{cal mol}^{-1}\text{K}^{-1}$	$4.184 \text{ J mol}^{-1}\text{K}^{-1}$
Number of moles of substance B	n_B		
Mole fraction of substance B: $n_B / \sum_i n_i$	x_B		
Chemical potential of substance B	μ_B	cal mol^{-1}	4.184 J mol^{-1}
Fugacity of substance B	f_B	bar	10^5 Pa
Activity of substance B	a_B		
Activity coefficient of substance B, mole fraction basis	γ_B^\dagger		
Stoichiometric coefficient of substance B	ν_B		
Site population number	α		
Excess parameters (Gibbs energy) of substance B	$\frac{W}{E}_B, \frac{W}{E}_{FB}$	cal mol^{-1}	4.184 J mol^{-1}
Excess parameter (volume) of substance B	$\frac{W}{V}_B$	cm^3	cm^3
Estimated standard error of quantity C	σ_C		
General equation for a chemical reaction	$0 = \sum_B \nu_B B$		
Gas constant	R	$\text{cal mol}^{-1}\text{K}^{-1}$	$4.184 \text{ J mol}^{-1}\text{K}^{-1}$

Compound	Symbol ^a	Formula Unit
Periclase	P	MgO
Brucite	B	Mg(OH, F) ₂
Intermediate sellaite	IS	Mg(OH, F) ₂
Sellaite	S	Mg(F, OH) ₂
Norbergite	N	Mg ₃ Si ₄ (OH, F) ₂
Chondrodite	Ch	Mg ₅ Si ₂ ⁰ ₈ (OH, F) ₂
Clinohumite	Cl	Mg ₉ Si ₄ ⁰ ₁₆ (OH, F) ₂
Forsterite	Fo	Mg ₂ SiO ₄
Enstatite	En	MgSiO ₃
Talc	Tc	Mg ₃ Si ₄ ⁰ ₁₀ (OH, F) ₂
Quartz	Qtz	SiO ₂
Water	H ₂ O	H ₂ O
Hydrogen fluoride	HF	HF

^a Prefixes of H and F are used with the symbols for the solid phases in order to denote the hydroxyl and fluorine endmembers respectively, e.g. HS refers to hydroxyl-sellaite and FCh to fluoro-chondrodite.

placing them in Stellite 25 or Rene 41 cold-seal pressure vessels (Tuttle, 1949) and nichrome-wound cylindrical furnaces. Temperature was controlled by a fully proportional controller with a platinum resistance sensing element. Temperatures were constantly monitored on a Texas Instruments twenty-four point Multiwriter recorder, and were measured at intervals of one to three days on a Leeds and Northrup K-3 potentiometer. Stainless steel sheathed chromel-alumel thermocouples were used for all temperature measurements. A standard thermocouple was calibrated against the melting points of NaCl (1073.5 K) and CsCl (919 K). Working thermocouples were calibrated against the standard with the pressure vessel in a position of minimum gradient in the furnace. Calibration is considered accurate to ± 2 K. Temperature variation over the bottom three centimeters of the pressure vessels was found to be less than 2 K.

Pressures were measured on Ashcroft Maxisafe Bourdon Tube gauges calibrated against a Heise Bourdon Tube gauge having a range of 0-7000 bar and an error of less than 7 bar. Individual pressure measurements are considered to be accurate to ± 20 bar.

Superscripts

⁰ is used to denote a property of a pure substance at a temperature of 1023 K and a pressure of 1 bar.

* is used to denote a property of a pure substance at some temperature, and/or pressure other than 1023 K and 1 bar.

T, P denotes a property at temperature T and pressure P .

Prefix

Δ , except when subscripted by R (see below), is used to denote a quantity of formation from the compounds MgO, MgF₂, SiO₂, H₂O, e.g., ΔG is the Gibbs energy of formation from the above compounds.

Subscripts

ex specifies an excess quantity, i.e., the difference between an actual quantity for a given solution phase and the value of that quantity in a corresponding ideal solution.

R indicates that the Δ -quantity refers to the difference for a reaction, i.e. $\Delta C_R = \sum_i \nu_i \Delta C_i$.

[†] The symbol γ has been used to represent the activity coefficient on a mole fraction basis rather than the recommended symbol f in order to avoid confusion between activity coefficient and fugacity.

Starting materials

The primary starting materials were Mallinckrodt Reagent MgF_2 lot MRC, Baker and Adamson Reagent MgO lot W196, and Fisher Certified Reagent Silicic Acid lot 730944. Before mixing, the MgF_2 was fired at 673 K for one hour. MgO was fired for 24 hours at 1300 K. Both the MgF_2 and MgO were allowed to cool in a desiccator with anhydrous CaSO_4 as the desiccant. The quantities of both materials required for the various mixes were then weighed out immediately. The silicic acid was fired at 1500 K for 24 hours to produce cristobalite. This was then crushed in an agate mortar and passed through a 100 mesh screen and stored in an oven at 423 K until weighed. Bulk compositions made up from these starting materials were ground in distilled water for two hours in an agate mortar and dried under a heat lamp before being loaded into run capsules.

Early attempts to use reagent-grade acetone as a grinding medium resulted in contamination of the mixes with a waxy residue, which resulted in the generation of CO_2 during the experiments and in some cases in the crystallization of magnesite or graphite.

Fluorine buffers

The fluorine buffers of Munoz and Eugster (1969) were examined for possible application to this system. It was found that buffers involving quartz could be used to buffer talc, but that other minerals in the system reacted with quartz in the buffers. The graphite-bearing buffers were generally found unsatisfactory because their use resulted in the crystallization

of carbonates; or, as in the case of the humites, the approach to equilibrium was extremely slow.

The (graphite-methane)-(wollastonite-fluorite-quartz) buffer was successfully used to buffer the F/OH ratio of talc. The fluid composition coexisting with this buffer was calculated as outlined by Munoz and Eugster (1969). Fugacity coefficients for H_2 were taken from Shaw and Wones (1964), and for H_2O from Burnham *et al.* (1969). The remaining fugacity coefficients were obtained by use of the Redlich-Kwong equation as described by Edminster (1968). Critical constants for methane were taken from American Society for Testing and Materials committee D-2 on petroleum products and lubricants and American Petroleum Institute research project 44 on hydrocarbons and related compounds (1971). The remainder of the critical constants were taken from Mathews (1972).

The remaining thermodynamic data used in the buffer calculations are listed, along with their sources, in Table 3. This data base differs significantly from that used by Munoz and Ludington (1974) and Munoz and Eugster (1969) with respect to the enthalpy of formation of fluorite from the elements. The value given by Stull and Prophet (1971) was adopted here over that of Robie and Waldbaum (1968) used by the above authors, because of its larger data base and better agreement with the experimental work of Bratland *et al.* (1970).

Solid phases

Synthesis and identification

Synthesis of the pure fluoro-humite endmembers was achieved at approximately one atmosphere in sealed platinum capsules. Attempts to synthesize such materials hydrothermally resulted in hydroxyl-bearing humites plus additional phases. All other phases were crystallized hydrothermally in sealed gold capsules.

Solid phases were identified primarily by means of X-ray powder diffraction. Standard patterns produced from single-phase synthesis products were particularly useful in the analysis of products consisting of mixtures of humites or of humites and forsterite, since the patterns for these minerals are quite similar.

Oil immersion methods were used as a secondary means of mineral identification, but positive optical distinction between the various humite minerals is extremely difficult in fine-grained run products. Optical techniques were used mainly to inspect for small amounts of extraneous phases in the run products.

Table 3. Thermodynamic data for the fluorine buffer

Compound	ΔH_f^{298} , elements (cal mol ⁻¹)	S^{298} (cal mol ⁻¹ K ⁻¹)	$C = a + b \cdot 10^{-3} T + c \cdot 10^5 / T^2$			V (cm ³)
			(cal mol ⁻¹ K ⁻¹)			
			a	b	c	
CaF_2	-293,000 ^a	16.39 ^a	14.30	7.28	0.47 ^b	24.558 ^c
CaSiO_3	-390,740 ^d	19.60 ^d	26.64	3.992	-6.517 ^e	39.93 ^c
$\alpha\text{-SiO}_2$	-217,700 ^a	9.91 ^a	10.495	9.277	-2.313 ^a	22.688 ^c
$\beta\text{-SiO}_2$			14.080	2.400	0.0 ^a	23.718 ^c
H_2O	-57,798 ^a	45.106 ^f	6.740	3.073	0.335 ^f	
HF	-65,140 ^a	41.508 ^a	6.529	0.657	0.231 ^a	

^a Stull and Prophet (1971)

^b Naylor (1945)

^c Robie, Bethke, and Beardsly (1967)

^d Robie and Waldbaum (1968)

^e Southard (1941)

^f Friedman and Haar (1954)

Characterization and compositional variation of phases

Cell dimensions were determined for all phases with variable fluorine-hydroxyl content except talc, for which only $d(060)$ was determined. The bulk composition of the solid phase was taken to be equal to that of the solid starting material plus H_2O . This is a good assumption, based upon the high degree of partitioning of fluorine into the solid phase and the fact that extrapolation of cell parameters from intermediate compositions to the fluorine endmembers gives good agreement with cell parameters determined for the fluoro-endmembers of the humite group when no fluid phase was present in the end-member synthesis. X-ray patterns of the materials used for the cell-dimension determinations showed only peaks for the material in question. Optical examination in no case revealed more than 2% extraneous material. It should, however, be borne in mind that a mixture of two humites could not reliably be detected optically.

X-ray patterns were made at a scan speed of 1/4 degree minute⁻¹. Silicon metal ($a = 5.4305A$) was used as the internal standard. Unit-cell parameters were refined using the program of Appleman and Evans (1973). Expressions for unit-cell parameters as a function of composition were then derived on the basis of a least-squares approximation. The coefficients for these equations are presented in Table 4, and the data upon which they are based in Appendix 1. Table 4 also shows end-member unit-cell parameters calculated from these relations and published unit-cell parameters for comparison. Unit-cell parameters of talc were not determined, because of overlap of the various peaks in the powder diffraction pattern.

Compositions of the phases in multiphase experiments were determined from the dependence on composition of interplanar spacing. These dependencies are based on measured d spacings in the case of talc and on calculated d spacings based on unit-cell refinements for the other phases. Coefficients for these equations appear in Table 5.

Peak positions were determined by oscillation against peaks of either silicon ($a = 5.4305A$) or spinel ($a = 9.0833A$) internal standards. Four measurements of $\Delta 2\theta$ were made at a scan speed of 1/4 degree per minute using Cu radiation and Ni filter.

For the phases of variable fluorine-hydroxyl content, excepting talc, molar volume-composition expressions have been computed by least squares. With the exception of brucite, all the volume functions are linear in composition. For sellaite and the humite

Table 4. Unit-cell parameters (A)

Phase	Unit cell parameter = $a+b \cdot x^a$				Fluoro-endmember		
	Space group	Param.	a	b	σ param. $\frac{b}{a}$	Calculated	Published
Sellaite		a_0	5.6185	-0.9929	$0.3 \cdot 10^{-2}$	4.626	4.623 ^c
Sp. gr. ?		b_0	4.3774	0.2474	$0.4 \cdot 10^{-3}$	4.625	4.623 ^c
		c_0	3.0507	-0.0006	$0.5 \cdot 10^{-4}$	3.050	3.052 ^c
	Norbergite	a_0	4.7168	-0.0098	$0.2 \cdot 10^{-4}$	4.707	4.709 ^d
Pbnm		b_0	10.3188	-0.0543	$0.1 \cdot 10^{-2}$	10.265	10.271 ^d
		c_0	9.0440	-0.3200	$0.8 \cdot 10^{-5}$	8.724	8.727 ^d
Chondrodite		a_0	4.7359	-0.0104	$0.1 \cdot 10^{-2}$	4.726	4.738 ^{d,e}
P2 ₁ /b		b_0	10.2778	-0.0306	$0.3 \cdot 10^{-2}$	10.247	10.278 ^{d,e}
		c_0	7.9526	-0.1615	$0.4 \cdot 10^{-2}$	7.791	7.813 ^{d,e}
		α	108.84	0.37	$0.8 \cdot 10^{-2}$	109.21	109.30 ^{d,e}
	Clinohumite	a_0	4.7469	-0.0066	$0.2 \cdot 10^{-2}$	4.740	4.751 ^{d,e}
P2 ₁ /b		b_0	10.2481	-0.0223	$0.1 \cdot 10^{-2}$	10.226	10.236 ^{d,e}
		c_0	13.7163	-0.1342	$0.1 \cdot 10^{-2}$	13.582	13.587 ^{d,e}
		α	100.59	0.35	$0.5 \cdot 10^{-1}$	100.94	100.88 ^{d,e}
Unit cell parameter = $a+b \cdot x+c \cdot x^2+d \cdot x^3$ $\frac{a}{b}$							
			a	b	c	d	σ param. $\frac{b}{a}$
Brucite		a_0	3.1464	-0.1776	0.0920		$0.5 \cdot 10^{-4}$
P $\bar{3}m1$		c_0	4.7694	-0.3525	1.7138	-2.5291	$0.2 \cdot 10^{-2}$
Description			a_0	b_0	c_0		
Calculated ($x=0.00^a$)			3.147		4.770		
Swanson et al. (1956)			3.147		4.769		
Description			a_0^f	b_0^f	c_0^f		
Intermediate sellaite	Coexisting with brucite		10.123(1)	4.6861(6)	3.0780(8)		
Pbnm or Pbn2 ₁ ^g	Coexisting with sellaite		10.097(6)	4.6812(19)	3.0738(25)		
	Crane and Ehlers (1969) ^e		10.122(2)	4.6845(13)	3.0801(4)		
Sellaite	Calculated ($x=0.50^a$)		5.122	4.5011	3.0504		

Note: ASTM Powder Diffraction File card 14-9 gives 13.68 as a_0 for FCl. This apparently should be modified to read 13.58. The Van Valkenburg (1961) FCh may well be a mixture of phases (probably two humites). The d -spacing of 3.897 listed by Van Valkenburg (1961) does not correspond to any possible d -spacing for a chondrodite with the space group and cell dimensions listed above.

^a x = mole fraction fluoro-endmember

^b The estimated standard errors have rather large uncertainties due to the small number of data points available (see appendix).

^c Swanson et al. (1955)

^d Van Valkenburg (1961)

^e Cell dimensions listed were calculated by means of the program of Evans, Appleman, and Handwerker (1963) from published d -spacings.

^f Numbers in parentheses are one estimated standard error in the digit to their immediate left.

^g Zero and first level c -axis Weissenburg diffraction patterns are consistent with an orthorhombic symmetry. The observed systematic extinctions are $h \ 0 \ l, \ h + l = 2n + 1$ and $0 \ k \ l, \ k = 2n + 1$.

Table 5. Variation of interplanar spacings with composition

Phase	$\bar{h} \ \bar{k} \ \bar{l}$	d-spacing (\AA) = $a+b \cdot x+c \cdot x^2 \frac{a}{d}$			
		a	b $\cdot 10$	c $\cdot 10$	$\sigma_d \frac{a}{b}$
Brucite	1 1 0	1.57318	-0.8873	0.4573	$0.3 \cdot 10^{-4}$
Sellaite	2 2 0	1.76085	-1.2555		$0.5 \cdot 10^{-3}$
Norbergite	1 2 1	3.11379	-0.5922		$0.5 \cdot 10^{-4}$
Norbergite	1 4 1	2.00072	-0.5757		$0.4 \cdot 10^{-4}$
Chondrodite	$\bar{1}$ 1 2	3.04133	-0.3810		$0.8 \cdot 10^{-3}$
Clinohumite	$\bar{5}$ 1 1	2.36875	-0.1724		$0.5 \cdot 10^{-3}$
Clinohumite	9 0 0	1.49801	-0.1628		$0.9 \cdot 10^{-4}$
Clinohumite	4 1 1	2.55580	-0.2176		$0.1 \cdot 10^{-3}$
Talc	0 6 0	1.52731	-0.0615		$0.7 \cdot 10^{-4}$

^a x = mole fraction fluoro-endmember.

^b The estimated standard errors have rather large uncertainties due to the small number of data points available (see appendix).

minerals the difference in volume between the hydroxyl and fluoro-endmembers is $2.95 \pm 0.19 \text{ cm}^3 \text{ mol}^{-1}$ of $(\text{OH})_2$. The volume of hydroxyl-talc has been taken from Robie *et al.* (1967) and that of fluoro-talc has been estimated as this value minus 2.95. The volume data are presented in Table 6.

Intermediate sellaitite, MgOHF

Crane and Ehlers (1969) synthesized a phase which they regarded as stoichiometric with a composition of MgOHF. The existence of this phase has been substantiated and its unit cell determined. Peaks were indexed on an orthorhombic unit cell from single-crystal Weissenberg radiographs. Final cell refinements were done as described for the other solid solution phases in the system. We suggest that this compound has a structure similar to that of sellaitite, with ordering of the fluorine and hydroxyl resulting in a doubling of the a dimension of the unit cell. It is therefore referred to here as intermediate sellaitite. Cell dimensions for intermediate sellaitite coexisting with sellaitite and with periclase, and those based on a refinement of the data of Crane and Ehlers (1969), are given in Table 4.

The inference that sellaitite and intermediate sellaitite are both members of a single structurally-continuous solid solution series is based upon measurement of cell parameters. Upon substitution of hydroxyl into the sellaitite structure, the symmetry changes from tetragonal to a lower symmetry, suggesting ordering of fluorine and hydroxyl. Cell parameters for sellaitite ($X_{\text{FS}} = 0.50$) are given in Table 4 for comparison with those of intermediate sellaitite.

This evidence leads to description of sellaitite and intermediate sellaitite by the same set of functions in the thermodynamic modelling which follows. For this reason special note should be made of the volume function for the sellaitite. The function given in Table 6 is based only on the data for sellaitite. The volume data for intermediate sellaitite has not been included, because the derivative of the volume with respect to composition is not closely constrained by the data at the intermediate sellaitite composition. The pressure effect upon equilibria involving intermediate sellaitite is therefore somewhat uncertain.

Experimental phase equilibrium results

Results of the experiments involving two or more phases for which the compositions have been determined are summarized in Table 7. With the exception of the data involving brucite, few of the equilibria depicted by these data are closely bracketed. This fact, combined with the generally long run times needed before apparent equilibrium was achieved, creates some uncertainty as to the closeness of approach to equilibrium. Metastability may also be a problem. In particular, experiment Ch100-C140-IR produced clinohumite considerably more fluorine-rich than is inferred to be truly stable. The experimental evidence does not resolve whether or not stable talc-clinohumite tie lines exist at 1023 K and 2000 bar. Experimental attempts to resolve this question were unsuccessful.

Table 6. Variation of molar volumes with composition

Phase A	$\bar{V} = x_{\text{FA}} \cdot \bar{V}_{\text{FA}}^{\text{O}} + x_{\text{HA}} \cdot \bar{V}_{\text{HA}}^{\text{O}} + x_{\text{FA}} \cdot x_{\text{HA}} \cdot \bar{W}_{\text{V,A}}$			
	$\bar{V}_{\text{FA}}^{\text{O}}$	$\bar{V}_{\text{HA}}^{\text{O}}$	$\bar{W}_{\text{V,A}}$	$\sigma_V \frac{a}{b}$
Brucite	25.732	24.621	-5.1897	$0.8 \cdot 10^{-2}$
Sellaite	19.649	22.789		$0.1 \cdot 10^{-1}$
Norbergite	63.466	66.293		$0.4 \cdot 10^{-2}$
Chondrodite	107.32	110.32		$0.4 \cdot 10^{-1}$
Clinohumite	194.64	197.49		$0.5 \cdot 10^{-1}$
Talc	133.30	136.25		

Note: All numbers are expressed in cubic centimeters.

^a The estimated standard errors have rather large uncertainties due to the small number of data points available (see appendix).

The requirement that all the equilibrium data and all the thermodynamic data be internally consistent is a stringent one that can be tested in the form of a number of simultaneous equations. In order to analyze the experimental data and to provide a basis for calculating other equilibria in the system and to calculate equilibria at conditions other than those of the experiments, a thermodynamic model of the system has been constructed based on such a system of equations.

The thermodynamic model

Introduction

The experimentally-determined phase equilibria represent a large number of constraints upon the thermodynamic properties of the system. Appendix 2 and 3² describe the development of a model that is consistent both with these data and with other phase equilibria and calorimetric data. Some parameters are not closely constrained by the phase equilibrium data. These have been evaluated from existing thermochemical data. The remaining parameters have been determined by means of a least-squares solution of a system of equations defined by the available phase equilibrium and thermochemical data.

The model is referenced to the components MgO, MgF₂, SiO₂, and H₂O, at 1023 K and 1 bar. The temperature of 1023 K has been chosen because much of the experimental evidence has been collected near this temperature. This choice simplifies the form of some of the equations to be used.

The method described in Appendix 3 evaluates 33 unknown thermodynamic parameters involved in the description and calculation of equilibria in this system. At a minimum, 33 equations would be needed to solve for these parameters. To the extent that an experiment reaches equilibrium, it represents at least one and usually several equations of constraint involving *P*, *T*, compositions, and free energy. Taken together, the models tested here involve an array of more than 70 equations, so that there are many more equations than unknowns. Since all involve measured quantities, none will be exact. The best approximation to satisfy all of the equations simultaneously has been sought by the method of least squares. This approach assumes that all of the measurements are normally distributed about the equilibrium values.

This assumption will only be true if all the assemblages measured have reached equilibrium, so that the only errors are those of measurement. Errors caused by failure of the experiments to reach equilibrium are difficult to treat, since their error distributions will be asymmetrical. The asymmetry arises because the experiments approach equilibrium from a particular direction and cannot pass through the equilibrium value. If only one equilibrium was studied and it was approached from only one direction, treatment by the method of least squares would result in an undetected bias in the results.

The data treated in this problem represent a large number of different equilibria which have been approached from different starting compositions. While lack of equilibrium may create problems in weighting the data, the fact that all the data can be described by a single model is strong evidence that all experiments considered have closely approached equilibrium. Preliminary experiments of short duration cannot be represented by any internally consistent model and have been omitted both from Table 7 and the thermodynamic analysis.

Testing of the alternative models

A test of any thermodynamic model is that it reproduce the experimental data within their uncertainties. Consequently it is necessary to calculate the conditions of various equilibria from the thermochemical quantities which constitute the model. The simplest of these calculations involves finding the composition of one solution phase in equilibrium with another solution phase of specified composition. This may be done at any pressure and temperature by appropriate manipulation of equation (46) or (47) of Appendix 3 with addition of terms containing heat capacities. Calculation of the equilibrium position of a four-phase field is more complex. In general it is necessary to solve a system of five equations simultaneously. Three independent equations, involving all three solid phases and the fluid phase, of the form of equation (46) or (47), with heat capacities, can be written. A fourth equation of the form of equation (48) can be written. Finally, since the fluid is present as a phase the equation

$$P = \sum_i f_i/\gamma_i \quad (1)$$

where the *i* are the various species in the fluid phase, may be written. Only three species, H₂O, HF, and H₂ are present in the fluid in appreciable amounts. H₂ is not involved in any of the equilibria considered, and therefore its only influence is as an inert component

² To obtain a copy of Appendices 2 and 3, order Document AM-79-110 from the Business Office, Mineralogical Society of America, 2000 Florida Avenue, N.W., Washington, D. C. 20009. Please remit \$1.00 in advance for the microfiche.

Table 7. Experimental results

Experiment number	T^a (K)	P^a (bar)	Duration (hour)	Starting materials b,c	Products a,b	$2 \cdot \ln(\frac{f_{H_2O}}{f_{HP}})$
Tc0-3R	1023(3)	2000(15)	1871	Tc0	Tc43.3(20)	14.93
Tc60-6R	1020(4)	1990(30)	1438	Tc60	Tc44.8(22)	14.99
N60-B25-1 $\frac{d$	1021(3)	2000(15)	954	N60+B25	N63.4(5)+B21.6(2)	
N80-B20-1 $\frac{d$	1021(3)	2000(15)	954	N80+B20	N71.6(4)+B22.9(4)	
N60-Ch100-1R	1023(3)	2000(15)	1462	N60+Ch100	N76.6(8)+Ch73.9(15)	
N50-2	1024(3)	1990(15)	984	N50 mix	N63.4(15)+Ch61.1(35)	
N80-Tc40-1R	1022(3)	2000(15)	1315	N80+Tc40	N83.9(6)+Tc46.4(31)+Ch	
N80-Tc20-1R	1022(3)	2000(15)	1315	N80+Tc20	N82.2(3)+Ch 79.7(37)+Tc43.3(56)	
N80-Tc60-1R	1022(3)	2000(15)	1315	N80+Tc60	N83.4(18)+Tc48.2(68)	
N100-Tc40-1R	1022(5)	2000(20)	1450	N100+Tc40	N89.1(15)+Tc50.4(34)	
N100-Tc60-1R	1022(3)	2000(15)	1315	N100+Tc60	N93.2(6)+Tc59.5(29)	
Ch60-Tc40-1R	1022(5)	2000(20)	1450	Ch60+Tc40	Ch64.7(8)+Tc34.6(23)	
N60-Tc60-1R	1022(3)	2000(15)	1315	N60+Tc60	Ch77.9(26)+Tc47.3(33)+N	
C160-BO-2	1023(3)	2000(15)	1665	Ch60+Fo +B0 mix	Ch39.5(54)+C131.7(27)+P	
Ch100-C140-1R	1023(3)	2000(15)	1665	Ch100+C140	Ch69.2(37)+C167.8(40)	
C140-Tc40-1R	1022(3)	2000(15)	1315	C140+Tc40	C157.4(28)+Tc30.3(40)	
C140-Tc20-1R+C160	1023(3)	2000(15)	1665	C140+Tc20 +Ch60+Fo	C154.3(18)+Tc22.1(49)	
C110-1	1024(3)	2000(20)	742	C110 mix	C128.9(35)+Fo+P	
C160-Tc0-1R	1022(3)	2000(15)	1077	Ch60+Tc0+Fo	Tc35.3(23)+Fo+En	
2B5-4	970(2)	2000(10)	1076	B17+P	B12.7(2)+P	
2B5-5	970(2)	2000(10)	1076	B5	B13.5(2)+P	
2B15-5	1023(3)	2000(15)	1459	B24+P	B22.3(4)+P	
1B15-18	1023(3)	2000(15)	1459	B15	B23.1(2)+P	
2B15-7	1047(3)	1990(15)	1352	B15	B24.6(2)+P	
2B15-8	1047(3)	1990(15)	1352	B25+P	B24.3(3)+P	
1B15-17	973(2)	1000(15)	1086	B15	B22.4(3)+P	
2B15-4	973(2)	1000(15)	1086	B25+P	B22.2(3)+P	
1B30-2	802(2)	2005(10)	423	B30 mix	B22.1(2)+IS	
1B30-5	970(2)	2000(10)	1076	B22+IS	B24.1(2)+IS	
1B30-6	970(2)	2000(10)	1076	B25+IS	B24.5(2)+IS	
1B30-3A	1022(3)	2000(15)	1077	B25+IS	B24.3(2)+IS	
1B30-1	1043(2)	1985(10)	146	B30 mix	B24.4(2)+IS	
1B30-3	1047(3)	1990(15)	1352	B30 mix	B25.6(2)+IS	
S75-1	827(2)	1990(10)	337	S75 mix	S89.1(4)+IS	
S75-5	970(2)	2000(10)	1076	S75 mix	S85.2(4)+IS	
S75-4	1022(3)	2000(15)	1077	S75 mix	S84.3(4)+IS	
S75-3	1047(3)	1990(15)	1352	S75 mix	S83.8(4)+IS	
S70-4	1070(2)	1990(10)	124	S70 mix	S83.3(2)+IS	
S75-4A	1070(2)	1990(10)	124	S75 mix	S83.0(2)+IS	

^a Numbers in parentheses are one estimated standard error in the digit to their immediate left.

^b The numbers which follow the mineral symbols are the mole percent fluoro-endmember. All starting materials include H₂O. All products include a vapor phase.

^c Mix refers to a mixture of the primary starting materials of the bulk composition indicated.

^d These experiments are not felt to have attained equilibrium, but they do bracket the composition of norbergite in equilibrium with brucite of composition $x_{FB}=0.22$.

in the fluid phase. Simultaneous solution of this non-linear set of equations provided the composition of all four coexisting phases. Note that such calculations may produce either stable or metastable assemblages. The method used to assess stability or metastability has been to inspect for four-phase fields which have a compositional volume in common, and to calculate which assemblage has the lower Gibbs energy for a given composition within that compositional volume. The assemblages having the lowest Gibbs energies when this procedure is carried out for all the calcu-

lated assemblages are assumed to be stable. The success of this procedure depends upon the set of stable four-phase assemblages being a subset of the set of assemblages being tested. The possibility that this condition may not be fulfilled exists because the method used to solve the system of equations outlined above requires a good initial estimate to achieve convergence. If a solution cannot be achieved for a given four-phase assemblage, it is not always obvious whether this is because a solution does not exist or because an unsuitable initial esti-

mate has been made. Nevertheless, the correspondence between the calculated assemblages and those observed both in the laboratory and in nature provides some confidence that the most stable assemblages have been found.

In order to evaluate the coefficients of equation (48) for those equilibria involving H₂O it has been assumed that the fluid phase is an ideal mixture of

H₂O, HF, and H₂, and that the dilution of H₂O by HF has a trivial effect upon ΔG_{H_2O} . The model is consistent with these assumptions. Figure 1, which shows the stable assemblages computed from the model at 2000 bar, shows that for all equilibria considered here f_{HF} is less than 2 bar. f_{H_2} has been estimated as 14 bar, based on the buffering effects of the pressure vessels. For a fluid so dominated by a single species

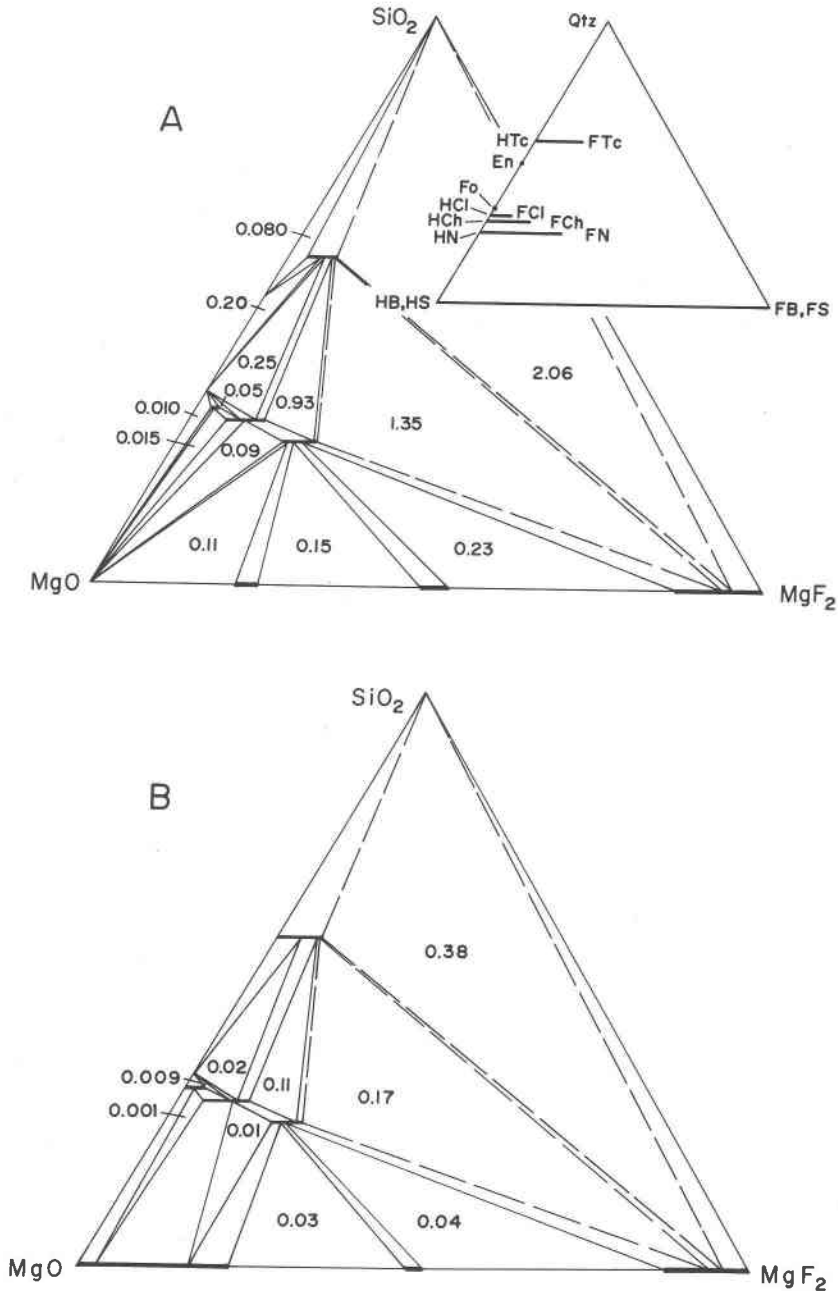


Fig. 1. The system MgO-MgF₂-SiO₂-H₂O projected from H₂O onto MgO-MgF₂-SiO₂. Numbers shown are f_{HF} for each three-phase field. (A) $T = 1023$ K, $P = 2000$ bar. (B) $T = 873$ K, $P = 2000$ bar.

Table 8. Comparison of experimental data with thermodynamic models

Experiment number	Solid phases	Composition of the solid solution phases (mole fraction fluoro-endmember)			
		Experimental	Models		
			Preferred	Symmetric	Ideal
N80-Tc40-1R	N	0.822(3)	0.819	0.822	0.857
	Tc	0.433(56)	0.462	0.421	0.498
	Ch	0.797(37)	0.788	0.749	0.817
N50-2	N	0.634(15)	0.638	0.543	0.556
	Ch	0.611(35)	0.593	0.441	0.482
	P				
C160-B0-2	Ch	0.395(54)	0.387	0.404	0.416
	Cl	0.317(27)	0.331	0.347	0.370
	P				
Ch60-Cl50-1R	Ch	0.535(26)	0.536	0.431	0.518
	Cl	0.483(9)	0.490	0.373	0.469
	Fo				
C110-1	Cl	0.289(35)	0.272	0.338	0.345
	Fo				
	P				
C160-Tc0-1R	Tc	0.353(23)	0.354	0.339	0.325
	Fo				
	En				
N60-B25-1 +N80-B20-1	B	0.220(0)	0.220	0.220	0.220
	N	0.670(40)	0.662	0.650	0.647
2B5-4	B	0.127(2)	0.130	0.126	0.089
	P				
2B5-5	B	0.135(2)	0.130	0.126	0.089
	P				
2B15-5	B	0.223(4)	0.214	0.214	0.229
	P				
1B15-18	B	0.231(2)	0.214	0.214	0.229
	P				
2B15-7	B	0.246(2)	0.249	0.248	0.287
	P				
2B15-8	B	0.243(3)	0.249	0.248	0.287
	P				
1B15-17	B	0.224(3)	0.228	0.231	0.258
	P				
2B15-4	B	0.222(3)	0.228	0.231	0.258
	P				
1B30-2	B	0.221(2)	0.221	0.221	0.222
	IS	0.490(20)	0.489	0.493	0.497
1B30-5	B	0.241(2)	0.237	0.238	0.238
	IS	0.490(20)	0.487	0.486	0.487
1B30-3A	B	0.243(2)	0.243	0.244	0.243
	IS	0.490(20)	0.487	0.484	0.485
1B30-6	B	0.245(1)	0.237	0.238	0.238
	IS	0.490(20)	0.487	0.486	0.487
1B30-1	B	0.244(2)	0.245	0.246	0.244
	IS	0.490(20)	0.487	0.483	0.484
1B30-3	B	0.256(2)	0.246	0.246	0.245
	IS	0.490(20)	0.487	0.483	0.484
S75-1	S	0.891(4)	0.880	0.868	0.868
	IS	0.510(20)	0.506	0.468	0.461
S75-5	S	0.852(4)	0.860	0.845	0.844
	IS	0.510(20)	0.523	0.489	0.482
S75-4	S	0.843(4)	0.855	0.836	0.835
	IS	0.510(20)	0.527	0.496	0.490
S75-3	S	0.838(4)	0.852	0.832	0.829
	IS	0.510(20)	0.529	0.501	0.495
S70-4	S	0.833(2)	0.850	0.828	0.825
	IS	0.510(20)	0.531	0.504	0.499
S74-4A	S	0.830(2)	0.850	0.828	0.825
	IS	0.510(20)	0.531	0.504	0.499

Table 8. (continued)

Phases in equilibrium	Pressure (bar)	Temperature (K)			
		Experimental	Preferred	Symmetric	Ideal
P,S,IS, fluid	1000	1038(15)	1042	978	957

Phase	ΔG° (cal mol ⁻¹)			
	Calorimetric	Models		
		Preferred	Symmetric	Ideal
HB	15550(226)	15538	15536	15231
Fo	-14213(338)	-14249	-12553	-11954
En	-7879(440)	-7566	-6834	-6598

Note: Numbers in parentheses are one estimated standard error in the digit to their immediate left.

the assumption of ideal mixing will be quite adequate for the most abundant species, but may be less satisfactory for the least abundant.

In order to find the simplest model that will describe the data, additional equations were added to represent linear combinations among the parameters. These equations were given sufficient weight that their residuals in no case exceed 0.1 cal mol⁻¹.

Initial solutions of the full least-squares problem produced excess parameters for the different humite phases which were equal within their uncertainties. This fact coupled with the structural similarity of the humites led to the addition of constraints that the excess parameters are identical for norbergite, chondrodite, and clinohumite. It has also been found possible to set the excess parameter 'E' equal to zero for all phases except sellaitite without detracting from the quality of the model. Setting E_s equal to zero produces parameters that deny the stable existence of intermediate sellaitite and predict that the hydroxyl-sellaitite endmember is more stable than the hydroxyl-brucite endmember, in contradiction of experimental evidence and natural occurrences. A non-zero E_s has therefore been retained. Such a model produces an acceptable description of the data, but suggests that W_{HB} and W_{FB} might be set equal. Such a model, with a symmetric solution for brucite, has been chosen as the simplest acceptable description of the system.

Two simpler models have also been treated. In the first all solid solutions other than sellaitite are modeled as symmetric. In the second they are modeled as ideal. The three models will be referred to as the preferred, symmetric, and ideal models. In Table 8 and Figures 2 and 3 the models are compared to the experimental data. The experimental data depicted in Figure 2C and 2D (equilibria [16] and [17], $X_{HTc} = 1$)

are largely from Chernosky (1976). These data were not available at the time the least-squares problem was formulated. The data used in formulation of the least-squares problem were from Chernosky (1974).

Many of the experimental data are nearly as well reproduced by the symmetric and ideal models as by the preferred. The major failures of the simpler models are in the prediction of the compositions of triplets of coexisting solid phases and of the Gibbs energies of forsterite and enstatite. In some of these cases the calculated values based upon the simpler models differ from the data by several estimated standard errors of the data.

Table 9 lists the parameters that represent the solution vector for the least-squares problems based on

the preferred model. The values for these parameters have been given to the nearest units place in spite of their rather large estimated standard errors. This has been done due to the high correlations between these parameters which are evident from examination of the matrix of correlation coefficients given in Table 10.

It is extremely important to be aware of the role played by the matrix of correlation coefficients. Parameters found by solution of the least-squares problem are not fully independent, being constrained to follow one another through their respective correlation coefficients. The important effect of this is that one is not free to specify arbitrary values for each parameter within its uncertainty, because this will deny the strong correlation that exists between the param-

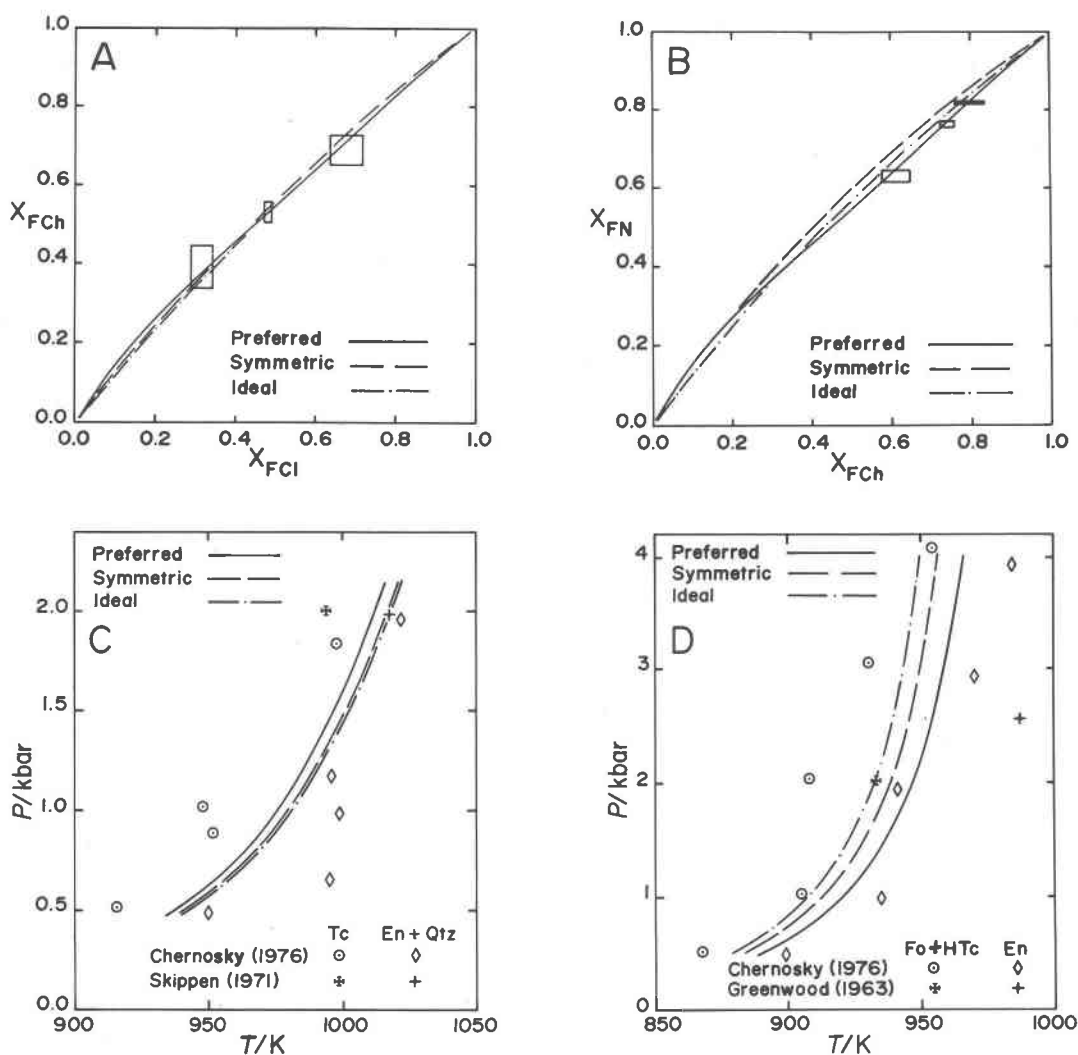


Fig. 2. Comparison of the preferred, symmetric, and ideal models with experimental data. Rectangles in A and B represent points within one σ of the experimental data. Points in C and D represent the maximum uncertainty in the experimental bracket. Note: These data are only a part of the total data. For a model to be acceptable it must conform to all the data.

eters and will result in a much inferior set of computed equilibrium conditions.

The parameters in Table 9 along with those listed in Table 11 may be used, within limits, to calculate phase equilibria in the system under a wide range of physical conditions. The most important limiting condition is probably the possible appearance of additional phases. If additional phases are stable, some of the calculated equilibria will be metastable. This may be a problem even at 1023 K and 2000 bar, due to the possible stability of anthophyllite. Discretion should also be exercised in using calculated equilibria at conditions other than those of the experiments. This is particularly true of other temperatures, due to the estimated nature of ΔS° and C for many of the endmember phases and because of the assumption that $\Delta S_{ex} = 0$ for all solution phases.

The position of the quartz–talc–sellaite–fluid and

talc–norbergite–sellaite–fluid fields is in doubt. No measurements of coexisting sellaite and talc compositions were possible, due to the interference of sellaite diffraction peaks with the (060) peak of talc. However, talc and norbergite more fluorine-rich ($X_{FTc} = 0.64$, $X_{FN} = 0.94$) than predicted by the model ($X_{FTc} = 0.50$, $X_{FN} = 0.84$) have been crystallized at 1023 K and 2000 bar. Several explanations for this discrepancy are possible. There is some textural evidence to suggest that a melt phase may have been present in these fluorine-rich experiments. The melt hypothesis offers an explanation only if the observed norbergite and talc are quench phases, since if they coexisted with the melt at the conditions of the experiment they should be more hydroxyl-rich than if no melt had been present. The textures are inconclusive regarding this possibility.

Two more probable possibilities are that the model

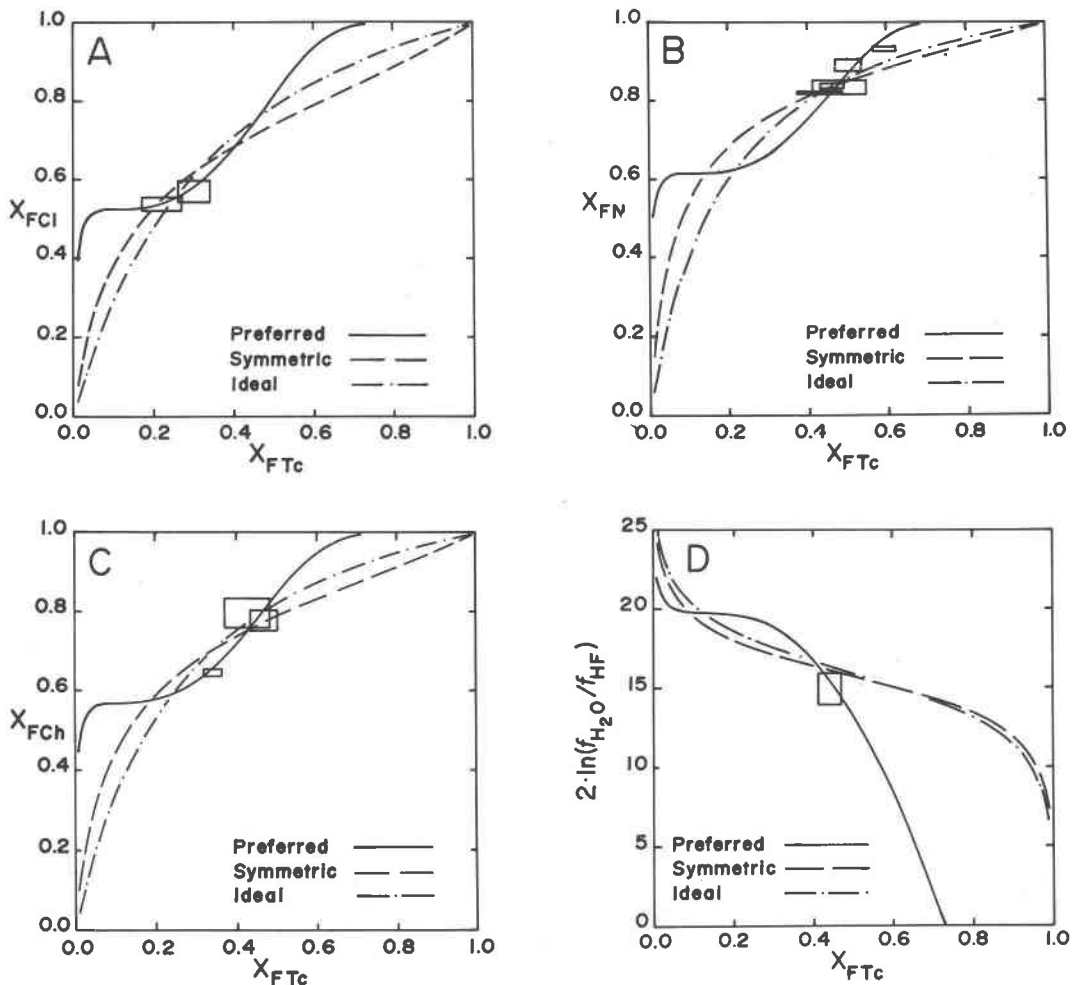


Fig. 3. Comparison of the preferred, symmetric, and ideal models with experimental data. Rectangles represent points within one σ of the experimental data. Note: These data are only a part of the total data. For a model to be acceptable it must conform to all the data.

does not adequately describe this portion of the system or that the high-fluorine norbergites and talcs are metastable. Inadequacy of the model in this region may arise from the treatment of the fluid phase as an ideal mixture of H₂O and HF. The model predicts that at 1023 K and 2000 bar f_{HF} in a fluid coexisting with norbergite with $X_{\text{FN}} = 0.94$ will be approximately 10 bar. For a talc with $X_{\text{FTc}} = 0.64$ f_{HF} is predicted to be about 70 bar. H₂O at these conditions has a specific volume of about 2 cm³ gram⁻¹ (Burnham *et al.*, 1969). At this density there is a possibility of polymerization in the HF-H₂O fluid which would lead to non-ideal mixing. With the increase in f_{HF} , SiF₄ may also become an important species in the fluid, especially if it coexists with quartz.

Applications

The thermodynamic model presented here is general enough to be of use in the analysis of a variety of mineralogic problems. There follows a small variety of applications to relatively simple problems.

Figure 4A is a T - X section at 2000 bar of the system MgO-MgF₂-H₂O projected from H₂O. Such a projection is not strictly legal (Greenwood, 1975), since H₂O is not present as a pure phase in this system. However, HF is the only other fluid species of importance; and, as may be seen from examination of Figure 4B, it makes up a very minor proportion of the fluid, except at very fluorine-rich bulk compositions. For this reason projections from H₂O on MgO-MgF₂-SiO₂ constitute adequate representations of the system MgO-MgF₂-SiO₂-H₂O.

The effect of fluorine on the upper stability of brucite is illustrated in Figure 4A. Similar information is presented in an alternative form in Figure 5. Displacement of equilibria involving talc and clinohumite are also presented in Figure 5. The error limits shown in this figure represent 2σ of the error derived from the error estimates of the least-squares parameters, accounting for covariance. These should provide reasonably accurate estimates of uncertainty within the range of the experimental conditions, but may tend to underestimate errors outside this range. If the model parameters are chosen within their own limits, but without regard for covariance, the errors in estimated positions are generally many times larger.

The importance of these figures in the interpretation of natural assemblages lies in the profound effect of fluorine substitution on the stability of

Table 9. Thermodynamic properties determined by least squares (preferred model)

Parameter ^a	Numerical Value	Estimated standard error
$\Delta G_{\text{HB}}^{\circ}$	15538	21
$\Delta G_{\text{FB}}^{\circ}$	8466	1332
$\Delta S_{\text{FB}}^{\circ}$	-31.7	1.6
$\frac{W_{\text{HB}}}{W_{\text{FB}}} = \frac{W_{\text{FB}}}{W_{\text{HB}}}$ ^b	-8396	541
$\Delta G_{\text{HS}}^{\circ}$	44092	23719
$\Delta S_{\text{HS}}^{\circ}$	0.9	1.1
$\frac{W_{\text{HS}}}{W_{\text{HS}}}$	-30341	32215
$\frac{W_{\text{FS}}}{W_{\text{FS}}}$	-145974	123278
E_{S}	141881	113066
$\Delta G_{\text{HN}}^{\circ}$	5333	1017
$\Delta G_{\text{FN}}^{\circ}$	-15721	1423
$\Delta G_{\text{HCh}}^{\circ}$	-12031	775
$\Delta G_{\text{FCh}}^{\circ}$	-31161	1662
$\Delta G_{\text{HCl}}^{\circ}$	-41347	1124
$\Delta G_{\text{FCl}}^{\circ}$	-58853	1881
$\frac{W_{\text{HN}}}{W_{\text{HCh}}} = \frac{W_{\text{HCh}}}{W_{\text{HCl}}} = \frac{W_{\text{HCl}}}{W_{\text{HCh}}}$ ^b	-14125	2250
$\frac{W_{\text{FN}}}{W_{\text{FCh}}} = \frac{W_{\text{FCh}}}{W_{\text{FCl}}} = \frac{W_{\text{FCl}}}{W_{\text{FCh}}}$ ^b	-5154	3669
$\Delta G_{\text{HTc}}^{\circ}$	-8509	401
$\Delta G_{\text{FTc}}^{\circ}$	-2086	2813
$\frac{W_{\text{HTc}}}{W_{\text{HTc}}}$	-56989	9276
$\frac{W_{\text{FTc}}}{W_{\text{FTc}}}$	-10239	2104
$\Delta G_{\text{Fo}}^{\circ}$	-14249	252
$\Delta G_{\text{En}}^{\circ}$	-7566	129

^a Δ -quantities are quantities of formation from MgO, MgF₂, SiO₂ and H₂O.

^b Excess parameters have been constrained to be equal.

hydroxyl-bearing minerals. It is vital to know to what extent the hydroxyl sites are occupied by fluorine. With such knowledge, the assemblage can be as informative as the equivalent assemblage involving the hydroxyl endmember.

Fluorine not only shifts the stabilities of hydroxyl minerals, but is also distributed between all the available hydroxyl sites in an assemblage of phases. Figure 4B illustrates the composition of the fluid that coexists with solid solutions of definite compositions. Since two solid solution phases in equilibrium with the same fluid must also be in equilibrium, at least metastably, with each other, this figure also provides information on the equilibrium compositions of coexisting solid solutions. The figure has been

Table 10. Matrix of correlation coefficients for properties in Table 9

Parameter	ΔG_{HB}^0	ΔG_{FB}^0	ΔS_{FB}^0	W_{HB}^a	ΔG_{HS}^0	ΔS_{HS}^0	W_{HS}	W_{FS}	E_S
ΔG_{HB}^0	1.000	0.212	0.009	-0.878	-0.010	0.068	0.009	0.010	-0.009
ΔG_{FB}^0	0.212	1.000	0.094	-0.246	-0.959	-0.001	0.915	0.951	-0.900
ΔS_{FB}^0	0.009	0.094	1.000	-0.009	-0.095	0.002	0.084	0.090	-0.082
W_{HB}^a	-0.878	-0.246	-0.009	1.000	0.015	-0.077	-0.014	-0.015	0.013
ΔG_{HS}^0	-0.010	-0.959	-0.095	0.015	1.000	-0.011	-0.980	-0.999	-0.970
ΔS_{HS}^0	0.068	-0.001	0.002	-0.077	-0.011	1.000	0.011	0.011	-0.010
W_{HS}	0.009	0.915	0.084	-0.014	-0.980	0.011	1.000	0.989	-0.999
W_{FS}	0.010	0.951	0.090	-0.015	-0.999	0.011	0.989	1.000	-0.982
E_S	-0.009	-0.900	-0.082	0.013	0.970	-0.010	-0.999	-0.982	1.000
ΔG_{HN}^0	0.000	-0.092	-0.009	0.001	0.095	0.002	-0.093	-0.095	0.092
ΔG_{FN}^0	-0.002	0.515	0.050	-0.002	-0.524	-0.011	0.500	0.519	-0.492
ΔG_{HCh}^0	0.000	-0.042	-0.004	0.000	0.044	0.001	-0.043	-0.044	0.043
ΔG_{FCh}^0	-0.001	0.438	0.043	-0.002	-0.446	-0.009	0.426	0.442	-0.419
ΔG_{HCl}^0	0.000	-0.005	-0.001	0.000	0.006	0.000	-0.007	-0.006	0.007
ΔG_{FCl}^0	-0.001	0.372	0.036	-0.002	-0.378	-0.008	0.361	0.375	-0.355
W_{HN}^a	0.000	0.126	0.012	-0.001	-0.130	-0.002	0.125	0.129	-0.123
W_{FN}^a	0.000	0.090	0.009	-0.001	-0.093	-0.001	0.090	0.092	-0.089
ΔG_{HTc}^0	0.000	0.020	0.002	0.000	-0.020	0.000	0.019	0.020	-0.018
ΔG_{FTc}^0	0.000	0.128	0.012	-0.001	-0.130	-0.002	0.124	0.129	-0.122
W_{HTc}	0.000	0.087	0.009	0.000	-0.089	-0.002	0.084	0.088	-0.083
W_{FTc}	0.000	0.090	0.009	0.000	-0.091	-0.002	0.087	0.090	-0.085
ΔG_{Fo}^0	0.000	0.022	0.002	0.000	-0.023	0.000	0.021	0.022	-0.021
ΔG_{En}^0	0.000	0.021	0.002	0.000	-0.021	0.000	0.020	0.021	-0.020

Table 10. (continued)

Parameter	ΔG_{HN}^0	ΔG_{FN}^0	ΔG_{HCh}^0	ΔG_{FCh}^0	ΔG_{HCl}^0	ΔG_{FCl}^0	W_{HN}^a	W_{FN}^a	ΔG_{HTc}^0
ΔG_{HB}^0	0.000	-0.002	0.000	-0.001	0.000	-0.001	0.000	0.000	0.000
ΔG_{FB}^0	-0.092	0.515	-0.042	0.438	-0.005	0.372	0.126	0.090	0.020
ΔS_{FB}^0	-0.009	0.050	-0.004	0.043	-0.001	0.036	0.012	0.009	0.002
W_{HB}^a	0.001	-0.002	0.000	-0.002	0.000	-0.002	-0.001	-0.001	0.000
ΔG_{HS}^0	0.095	-0.524	0.044	-0.446	0.006	-0.378	-0.130	-0.093	-0.020
ΔS_{HS}^0	0.002	-0.011	0.001	-0.009	0.000	-0.008	-0.002	-0.001	0.000
W_{HS}	-0.093	0.500	-0.043	0.426	-0.007	0.361	0.125	0.090	0.019
W_{FS}	-0.095	0.519	-0.044	0.442	-0.006	0.375	0.129	0.092	0.020
E_S	0.092	-0.492	0.043	-0.419	0.007	-0.355	-0.123	-0.089	-0.018
ΔG_{HN}^0	1.000	-0.243	0.842	-0.362	0.562	-0.171	-0.786	-0.959	0.213
ΔG_{FN}^0	-0.243	1.000	-0.061	0.902	0.091	0.804	0.310	0.301	0.191
ΔG_{HCh}^0	0.842	-0.061	1.000	-0.076	0.906	0.168	-0.397	-0.717	0.618
ΔG_{FCh}^0	-0.362	0.902	-0.076	1.000	0.157	0.911	0.459	0.449	-0.307
ΔG_{HCl}^0	0.562	0.091	0.906	0.157	1.000	0.410	-0.092	-0.370	0.849
ΔG_{FCl}^0	-0.171	0.804	0.168	0.911	0.410	1.000	0.355	0.308	0.517
W_{HN}^a	-0.786	0.310	-0.397	0.459	-0.092	0.355	1.000	0.774	0.131
W_{FN}^a	-0.959	0.301	-0.717	0.449	-0.370	0.308	0.774	1.000	0.001
ΔG_{HTc}^0	0.213	0.191	0.618	0.307	0.849	0.517	0.131	0.001	1.000
ΔG_{FTc}^0	0.330	0.211	0.181	0.026	0.087	-0.002	-0.448	-0.287	0.052
W_{HTc}	-0.328	0.202	-0.107	0.383	0.032	0.414	0.500	0.315	0.097
W_{FTc}	-0.332	0.206	-0.111	0.388	0.029	0.422	0.499	0.320	0.112
ΔG_{Fo}^0	0.227	0.206	0.665	0.331	0.913	0.554	0.155	0.000	0.932
ΔG_{En}^0	0.220	0.199	0.642	0.320	0.882	0.537	0.141	0.001	0.991

Table 10. (continued)

Parameter	ΔG_{FTc}^0	W_{HTc}	W_{FTc}	ΔG_{Fo}^0	ΔG_{En}^0
ΔG_{HB}^0	0.000	0.000	0.000	0.000	0.000
ΔG_{FB}^0	0.128	0.087	0.090	0.022	0.021
ΔS_{FB}^0	0.012	0.009	0.009	0.002	0.002
W_{HB}^a	-0.001	0.000	0.000	0.000	0.000
ΔG_{HS}^0	-0.130	-0.089	-0.091	-0.023	-0.021
ΔS_{HS}^0	-0.002	-0.002	-0.002	0.000	0.000
W_{HS}	0.124	0.084	0.087	0.021	0.020
W_{FS}	0.129	0.088	0.090	0.022	0.021
E_S	-0.122	-0.083	-0.085	-0.021	-0.020
ΔG_{HN}^0	0.330	-0.328	-0.332	0.227	0.220
ΔG_{FN}^0	0.211	0.202	0.206	0.206	0.199
ΔG_{HCh}^0	0.181	-0.107	-0.111	0.665	0.642
ΔG_{FCh}^0	0.026	0.383	0.388	0.331	0.320
ΔG_{HCl}^0	0.087	0.032	0.029	0.913	0.882
ΔG_{FCl}^0	-0.002	0.414	0.422	0.554	0.537
W_{HN}^a	-0.448	0.500	0.499	0.155	0.141
W_{FN}^a	-0.287	0.315	0.320	0.000	0.001
ΔG_{HTc}^0	0.052	0.097	0.112	0.932	0.991
ΔG_{FTc}^0	1.000	-0.882	-0.851	0.016	0.044
W_{HTc}	-0.882	1.000	0.974	0.124	0.105
W_{FTc}	-0.851	0.974	1.000	0.123	0.120
ΔG_{Fo}^0	0.016	0.124	0.123	1.000	0.967
ΔG_{En}^0	0.044	0.105	0.120	0.967	1.000

^a $W_{HB} = W_{FB}$, $W_{HN} = W_{HCh} = W_{HCl}$, $W_{FN} = W_{FCh} = W_{FCl}$, see

Table 13.

calculated for the specific conditions of 1023 K and 2000 bar. Numbers given for the fluid change markedly with temperature, but only slightly with pressure. In contrast, the compositions of coexisting solid solutions are rather insensitive to changes in temperature and pressure, rendering them unsatisfactory as geothermometers or barometers, but valuable as a test of equilibration between natural mineral pairs.

Bourne (1974) has analyzed coexisting pairs of phlogopite and clinohumite or chondrodite from natural assemblages. Error estimates of 0.05 in mole fraction fluoro-endmember have been applied to these data, which are compared in Figure 6 to the calculated equilibrium distributions utilizing the models presented here and an assumed ideal solution model for phlogopite based on the data of Munoz and Ludington (1974). The two curves presented for each mineral pair reflect the different enthalpies of

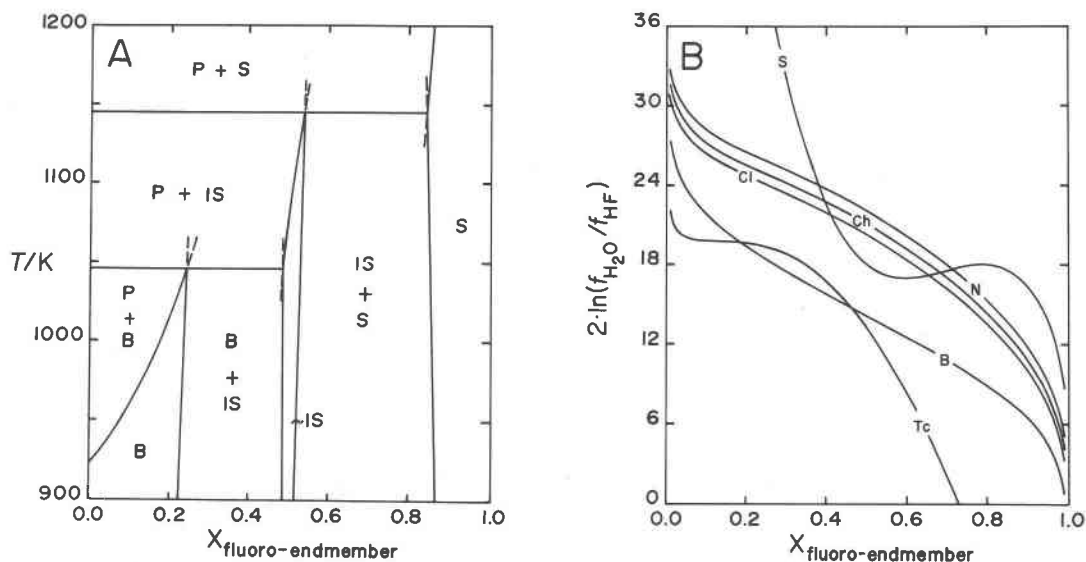


Fig. 4. (A) T - X section at 2000 bar of the system $\text{MgO-MgF}_2\text{-H}_2\text{O}$ projected from H_2O onto MgO-MgF_2 . (B) Plot of $f_{\text{H}_2\text{O}}$ to f_{HF} ratio vs. the compositions of the solid solution phases in the system at 1023 K and 2000 bar.

formation of fluorite discussed earlier and their effect on the fluorine buffer calculation.

The good correspondence between observed and calculated distributions indicates a close approach to equilibrium in the natural assemblages, but, because of the insensitivity of the distribution coefficients to pressure and temperature, it provides no information on geothermometry or barometry.

Bourne (1974) found no humite in any of the natural assemblages collected from a variety of locations. This finding is in agreement with the experimental results of this study. The compositions of the one pair of coexisting norbergite and chondrodite ($X_{\text{FN}} = 0.74$, $X_{\text{FCh}} = 0.72$) agree well with the model.

Stable assemblages in the system $\text{MgO-MgF}_2\text{-SiO}_2\text{-H}_2\text{O}$ at 1023 and 873 K and 2000 bar are presented in Figure 1. These provide insight into the limited compositional ranges of naturally-occurring minerals of the humite group. The combined data of Bourne (1974) and Jones *et al.* (1969) provide analyses for 5 norbergites, 38 chondrodites, and 12 titanium-poor clinohumites. From these data the most fluorine-rich norbergite reported is 98 mole percent fluoro-norbergite. According to the model, at temperatures less than 1300 K such a norbergite would not be stable at a pressure of H_2O greater than 100 bar. It should be born in mind, however, that this prediction rests on the potentially unreliable portion of the model. The most fluorine-rich natural chon-

drodite ($X_{\text{FCh}} = 0.82$) corresponds closely to the model prediction at 1100 K and 100 bar H_2O pressure. The insensitivity of maximum X_{FCh} to temperature at constant pressure ($2 \cdot 10^{-4} \text{ K}^{-1}$) suggests that chondrodites with $X_{\text{FCh}} > 0.82$ could crystallize only with $P_{\text{H}_2\text{O}} < 1000$ bar from very fluorine-rich bulk compositions. The non-occurrence of such chondrodites is probably due to the combined rarity of these conditions and bulk compositions. Such chondrodites could not coexist with quartz, due to the stability of talc, nor with magnesite or dolomite, due to the stability of norbergite. The most fluorine-rich natural clinohumite ($X_{\text{FCI}} = 0.61$) corresponds well to the predicted upper limit of X_{FCI} for the assemblage forsterite-chondrodite-clinohumite.

The lower limits of X_{F} for the humite minerals predicted by the model are generally lower than those of the observed natural minerals. For norbergite and chondrodite the lower limit of fluorine content is specified by the brucite-norbergite-chondrodite and brucite-chondrodite-clinohumite equilibria respectively. These do not involve the fluid phase and are therefore relatively insensitive to pressure and temperature variation. They explain reasonably well the lower observed limits of X_{FN} and X_{FCh} . The model predicts the stable existence of hydroxyl-clinohumite, but this phase has not been found in natural assemblages, nor has it been crystallized experimentally. This discrepancy is

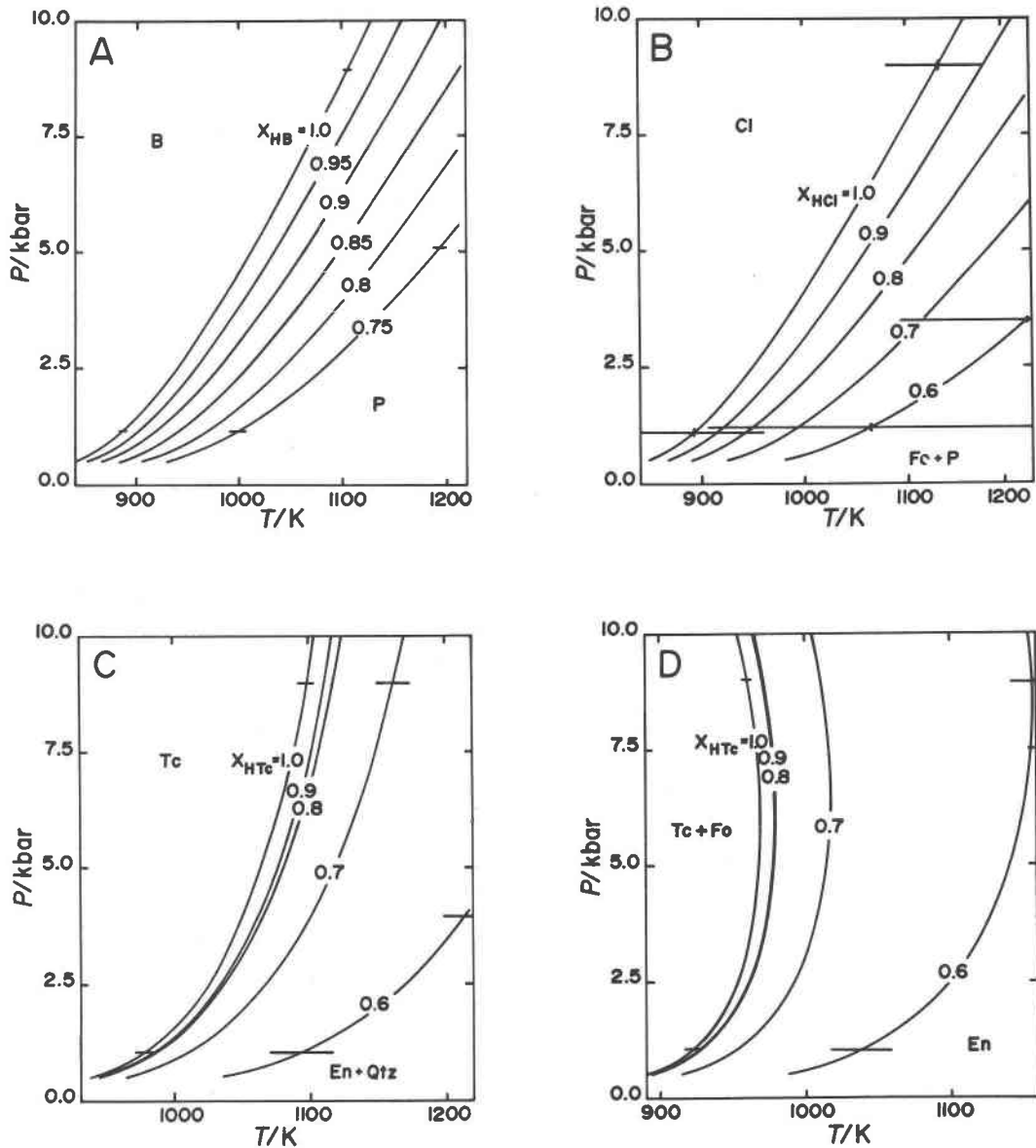


Fig. 5. Displacement of equilibria by variation in fluorine content of solid solution phases. (A) $HB = P + H_2O$. (B) $HCl = 4Fo + P + H_2O$. (C) $HTc = 3En + Qtz + H_2O$. (D) $HTc + Fo = 5En + H_2O$. Error bars represent 2σ in the temperature position of the equilibrium curves based upon the error estimates provided by the preferred model. Note: The Gibbs energy function for H_2O given by Holloway *et al.* (1971) was used in calculating these equilibria.

probably a consequence of uncertainties in the least-squares parameters. Within the error limits of the model, it is possible that the dehydration temperature of hydroxyl-clinohumite is lower than that of hydroxyl-brucite. If this is the case, the lower limit of X_{FCI} would be constrained by the brucite-clinohumite-forsterite equilibrium and pure hydroxyl-clinohumite would be unstable.

Conclusions

A model has been constructed for the system $MgO-MgF_2-SiO_2-H_2O$ which is in good agreement with available experimental and field data, except perhaps at the very fluorine-rich bulk compositions. The correspondence between theoretical and natural phase assemblages encourages confidence in the model. The model, besides being of specific value to

Table 11. Thermodynamic data evaluated prior to solution of the least-squares problem

Compound	$S_{298,1}^{298,1}$ (cal mol ⁻¹ K ⁻¹)	$C=a+b \cdot T+c/T^2$ (cal mol ⁻¹ K ⁻¹)			$V_{298,1}^{298,1}$ (cm ³)
		a	b · 10 ³	c · 10 ⁻⁵	
		P	6.44 ^b	11.358	
HB	15.09 ^e	26.117	1.501	-7.550 ^f	24.261 ^g
FB		16.511	2.931	-1.781 ^h	25.732 ^g
HS		26.117	1.501	-7.550 ^h	22.789 ^g
FS	13.68 ⁱ	16.511	2.931	-1.781 ^j	19.649 ^g
HN	36.52 ^k	64.182	6.410	-19.519 ^h	66.239 ^g
FN	36.39 ^k	54.576	7.840	-13.750 ^h	63.466 ^g
HCh	59.36 ^k	102.247	11.319	-31.488 ^h	110.32 ^g
FCh	59.13 ^k	92.641	12.749	-25.719 ^h	107.32 ^g
HCl	104.52 ^k	178.377	21.137	-55.426 ^h	197.49 ^g
FCl	104.38 ^k	168.771	22.567	-49.657 ^h	194.64 ^g
HTc	62.33 ^l	110.229	14.213	-39.916 ^h	136.25 ^g
FTc	61.99 ^m	100.623	15.643	-34.147 ^h	133.30 ^g
Fo	22.7 ⁿ	38.065	4.909	-11.969 ^o	43.786 ^g
En	16.2 ⁿ	24.245	5.020	-5.633 ^p	31.44 ^g
α-Qtz	9.91 ^q	10.495	9.277	-2.313 ^p	22.688 ^g
β-Qtz		14.080	2.400	0.000 ^p	23.718 ^g
H ₂ O	45.106 ^r	6.740	3.073	0.335 ^q	
HF	41.508 ^p	6.529	0.657	0.231 ^p	
ΔG° (cal mol ⁻¹)					
HF	10753	b, c, i, j, p, q, r			

^a Where the experimental data was available in the literature, a, b, and c were derived from that data by the method of least squares.
^b Barron, Berg, and Morrison (1959)
^c Victor and Douglas (1963)
^d Robie, Bethke, and Beardsley (1967)
^e Ciauaque and Archibald (1937)
^f King, Ferrante, and Pankratz (1975)
^g This paper
^h Estimated as the appropriate summation of C_{Fo} , C_{HB} , C_{FS} , and C_P
ⁱ Todd (1949)
^j Naylor (1945)
^k Estimated as the appropriate summation of S_{Fo}^{298} , S_{HB}^{298} , and S_{FS}^{298} with a volume correction as described by Fyfe, Turner, and Verhoogen (1958)
^l Robie and Stout (1963)
^m Estimated as $S_{HTc}^{298} - S_{HB}^{298} + S_{FS}^{298} + (V_{FTc} - V_{HTc} + V_{HB} - V_{FS}) (0.6)$
ⁿ Kelley (1943), S_{En}^{298} estimated as equal to S_{En}^{298} for clinoenstatite.
^o Orr (1953)
^p Stull and Prophet (1971), C_{En} estimated as equal to that for clinoenstatite.
^q Friedman and Haar (1954)
^r $\Delta H_{298,1}^{298,1}$ of formation from the elements equals -144,000 cal mol⁻¹, personal communication B. S. Hemingway (U.S. Geological Survey, Reston, Virginia).

Table 12. Equilibria that simultaneously constrain the thermodynamic model

[2] HB+FN=FB+HN	[11] 2HCh=P+HCl+H ₂ O
[3] HN+FCh=FN+HCh	[12] 2HN=P+HCh+H ₂ O
[4] HN+FTc=FN+HTc	[13] 14HN+HTc=9HCh+6H ₂ O
[5] HCh+FTc=FCh+HTc	[14] HB=P+H ₂ O
[6] HCh+FCl=FCh+HCl	[15] HIS=P+H ₂ O
[7] HCl+FTc=FCl+HTc	[16] HTc-3En+Qtz+H ₂ O
[8] HTc+2HF=FTc+2H ₂ O	[17] HTc+Fo=5En+H ₂ O
[9] 2Fo+HCh=HCl	[18] HB+FIS=FB+HIS
[10] HCl=P+4Fo+H ₂ O	[19] HS+FIS=FS+HIS

Table 13. Constraining phase equilibrium data from other sources

Phases in equilibrium	T (K) ^a	P (bar) ^a	Reference
IS, S, P, H ₂ O	1038(15)	1000(15)	Crane and Ehlers (1969)
HTc, Fo, En, H ₂ O	890(5) 911(5) 935(5) 952(5) 969(5)	500 1000 2000 3000 4000	Chernosky (1974)
HTc, En, Qtz, H ₂ O	933(5) 970(5) 1011(5)	500 1000 2000	Chernosky (1974)

^a Numbers in parentheses are one estimated standard error in the digit to their immediate left.

Table 14. Equations constraining single model parameters

Equation ^a	References
[48] $\Delta G_{HB}^\circ = 15550(226)$ cal mol ⁻¹	1, 2, 3, 4, 5, 6
[49] $\Delta G_{Fo}^\circ = -14213(338)$ cal mol ⁻¹	4, 5, 7, 8, 9, 10
[50] $\Delta G_{En}^\circ = -7879(440)$ cal mol ⁻¹	4, 5, 7, 8, 10

^a Numbers in parentheses are one estimated standard error in the digit to their immediate left.

- Taylor and Wells (1938)
- Ciauaque and Archibald (1937)
- King, Ferrante, and Pankratz (1975)
- Victor and Douglas (1963)
- Barron, Berg, and Morrison (1959)
- Friedman and Haar (1954)
- Charlu, Newton, and Kleppa (1975)
- Kelley (1943)
- Orr (1953)
- Stull and Prophet (1971)

understanding the system under study, should provide an outline of a general approach suitable for dealing with dehydration and exchange equilibria in a variety of experimental and natural systems.

Several equilibria present themselves as being fruitful areas for further study. In particular the equilibria involving talc, norbergite, sellaite, and quartz beg further study to clarify the nature of the

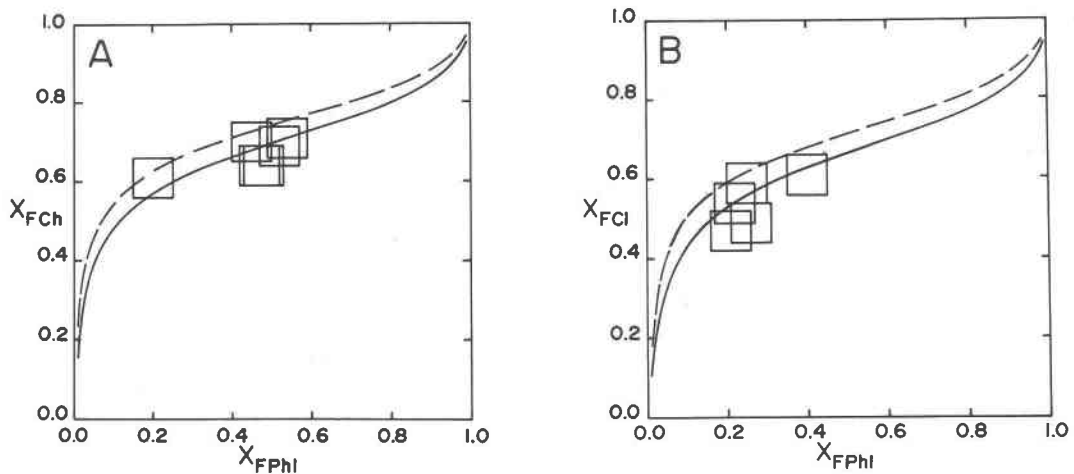


Fig. 6. Partitioning of fluorine and hydroxyl between phlogopite and chondrodite and between phlogopite and clinohumite. Squares represent points within 0.05 of the data for natural assemblages. The dashed lines are the relationships calculated using the data of Robie and Waldbaum (1968) for the enthalpy of fluorite in the buffer calculation to characterize the phlogopite solid solution. The solid lines have been calculated using the enthalpy of fluorite from Stull and Proppert (1971).

fluorine-rich portion of the system. This information may not be of great immediate geologic interest, but it may contribute indirectly to the improvement of the model as a whole. The talc–enstatite–quartz–fluid and talc–enstatite–forsterite–fluid equilibria may contribute to refinement of the talc solid solution model. Substantial improvements might be made in the description of clinohumite through study

of the brucite–clinohumite–forsterite and periclase–clinohumite–forsterite–fluid equilibria.

Acknowledgments

This work was supported through National Research Council of Canada grant A-4222 to H. J. Greenwood and by a U.S. National Science Foundation Graduate Fellowship, 1969–1971. Krista Scott assisted with the Weissenberg work on intermediate sellaitite.

Appendix I. Measured cell parameters of solid-solution phases

Phase	x^a	a_0 (Å)	b_0 (Å)	c_0 (Å)	α (°)	v (cm ³)
Sellaite	1.00	4.6249(4)	4.6249(4)	3.0502(3)		19.646(3)
Sp. gr. ?	0.90	4.7270(7)	4.5997(6)	3.0502(4)		19.971(4)
	0.85	4.7731(9)	4.5879(6)	3.0503(3)		20.115(4)
Brucite	0.00	3.1464(2)		4.7695(7)		24.627(4)
P3ml	0.05	3.1377(3)		4.7556(6)		24.419(4)
	0.15	3.1218(2)		4.7466(5)		24.126(3)
	0.15	3.1218(3)		4.7469(6)		24.129(4)
	0.20	3.1146(3)		4.7469(9)		24.018(5)
	0.25	3.1077(2)		4.7490(5)		23.921(4)
Norbergite	1.00	4.7072(5)	10.2650(9)	8.7240(10)		63.469(8)
Pbnm	0.90	4.7085(10)	10.2691(21)	8.7562(22)		63.746(18)
	0.70	4.7108(10)	10.2808(15)	8.8200(19)		64.315(15)
Chondrodite	1.00	4.7247(9)	10.2490(9)	7.7880(18)	109.2(2)	107.232(23)
P2 ₁ /b	1.00	4.7264(8)	10.2477(8)	7.7907(13)	109.2(2)	107.297(17)
	0.80	4.7263(7)	10.2512(9)	7.8279(13)	109.1(2)	107.896(18)
	0.80	4.7285(14)	10.2542(16)	7.8220(27)	109.1(3)	107.900(37)
	0.70	4.7287(13)	10.2519(15)	7.8398(22)	109.1(3)	108.148(30)
	0.60	4.7293(4)	10.2727(4)	7.8573(15)	109.1(2)	108.620(18)
Clinohumite	1.00	4.7396(12)	10.2259(33)	13.5819(31)	100.9(5)	194.630(74)
P2 ₁ /b	0.50	4.7450(19)	10.2356(121)	13.6497(50)	100.8(8)	196.099(210)
	0.40	4.7428(17)	10.2396(50)	13.6619(34)	100.7(5)	196.316(92)

Note: Numbers in parentheses are one estimated standard error in the digit to their immediate left.

^a x = mole fraction fluoro-endmember.

References

- American Society for Testing and Minerals committee D-2 on petroleum products and lubricants, and American Petroleum Institute research project 44 on hydrocarbons and related compounds (1971) *Physical Constants of Hydrocarbons C₁ to C₁₀*. American Society for Testing and Materials, New York.
- Appleman, D. E. and H. T. Evans, Jr. (1973) Job 9214: Indexing and least squares refinement of powder diffraction data. *Natl. Tech. Inf. Serv., U. S. Dep. Commerce*, Springfield, Virginia, Document PB-216 188.
- Barron, T. H. K., W. T. Berg and J. A. Morrison (1959) On the heat capacity of crystalline magnesium oxide. *Proc. R. Soc. Lond., A250*, 70–83.
- Bevington, P. R. (1969) *Data Reduction and Error Analysis for the Physical Sciences*. McGraw-Hill, New York.
- Bourne, J. H. (1974) *The Petrogenesis of the Humite Group Minerals in Regionally Metamorphosed Marbles of the Grenville Supergroup*. Ph.D. Thesis, Queen's University, Kingston, Ontario.
- Bratland, D., A. Fekri, K. Grjotheim and K. Motzfeldt (1970) Vapor pressure of silicon tetrafluoride above mixtures of fluorides and silica, I. The system CaF₂-SiO₂. *Acta Chem. Scand.*, 24, 864–870.
- Burnham, C. W., J. R. Holloway and N. F. Davis (1969) Thermodynamic properties of water to 1000°C and 10,000 bars. *Geol. Soc. Am. Spec. Pap.* 132.
- Charlu, T. V., R. C. Newton and O. J. Kleppa (1975) Enthalpies of formation at 970 K of compounds in the system MgO-Al₂O₃-SiO₂ from high temperature solution calorimetry. *Geochim. Cosmochim. Acta*, 39, 1487–1497.
- Chernosky, J. V., Jr. (1974) The stability field of anthophyllite—an experimental redetermination (abstr.). *Geol. Soc. Am. Abstracts with Programs*, 6, 687.
- (1976) The stability of anthophyllite—a reevaluation based on new experimental data. *Am. Mineral.*, 61, 1145–1155.
- Crane, R. L. and E. G. Ehlers (1969) The system MgF₂-MgO-H₂O. *Am. J. Sci.*, 267, 1105–1111.
- Edminster, W. C. (1968) Applied hydrocarbon thermodynamics, part 32, compressibility factors and fugacity coefficients from the Redlich-Kwong equation of state. *Hydrocarbon Processing*, 47, 239–244.
- Friedman, A. S. and L. Haar (1954) High-speed machine computation of ideal gas thermodynamic functions. I. Isotopic water molecules. *J. Chem. Phys.*, 22, 2051–2058.
- Fyfe, W. S., F. J. Turner and J. Verhoogen (1958) Metamorphic reactions and metamorphic facies. *Geol. Soc. Am. Mem.* 73.
- Giauque, W. F. and R. C. Archibald (1937) The entropy of water from third law of thermodynamics. The dissociation pressure and calorimetric heat of the reaction Mg(OH)₂ = MgO + H₂O. The heat capacities of Mg(OH)₂ and MgO from 20 to 300°K. *J. Am. Chem. Soc.*, 59, 561–569.
- Golub, G. H. and C. Reinsch (1970) Singular value decomposition and least squares solutions. *Numerische Mathematik*, 14, 403–420.
- Greenwood, H. J. (1963) The synthesis and stability of anthophyllite. *J. Petrol.*, 4, 317–351.
- (1975) Thermodynamically valid projections of extensive phase relationships. *Am. Mineral.*, 60, 1–8.
- Guggenheim, E. A. (1952) *Mixtures*. Clarendon Press, London.
- Holloway, J. R., D. H. Egger and N. F. Davis (1971) Analytical expression for calculating the fugacity and free energy of H₂O to 10,000 bars and 1300°C. *Geol. Soc. Am. Bull.*, 82, 2639–2642.
- Jones, N. W., P. H. Ribbe and G. V. Gibbs (1969) Crystal chemistry of the humite minerals. *Am. Mineral.*, 54, 391–411.
- Kelley, K. K. (1943) Specific heats at low temperature of magnesium orthosilicate and magnesium metasilicate. *J. Am. Chem. Soc.*, 65, 339–341.
- King, E. G., M. J. Ferrante and L. B. Pankratz (1975) Thermodynamic data for Mg(OH)₂ (brucite). *U. S. Bur. Mines. Rep. Invest.* 8041.
- Lawson, C. L. and R. J. Hanson (1974) *Solving Least Squares Problems*. Prentice-Hall, Englewood Cliffs, New Jersey.
- Maier, C. B. and K. K. Kelley (1932) An equation for the representation of high temperature heat content data. *J. Am. Chem. Soc.*, 54, 3243–3246.
- Mathews, J. F. (1972) The critical constants of inorganic substances. *Chem. Rev.*, 72, 71–100.
- McGlashan, M. L. (1970) Manual of symbols and terminology for physicochemical quantities and units. *Pure Appl. Chem.*, 21, 1–44.
- Muan, A. (1967) Determination of thermodynamic properties of silicates from locations of conjugation lines in ternary systems. *Am. Mineral.*, 52, 797–804.
- Munoz, J. L. and H. P. Eugster (1969) Experimental control of fluorine reactions in hydrothermal systems. *Am. Mineral.*, 54, 943–959.
- and S. D. Ludington (1974) Fluorine-hydroxyl exchange in biotite. *Am. J. Sci.*, 274, 396–413.
- Naylor, B. F. (1945) Heat contents at high temperatures of magnesium and calcium fluorides. *J. Am. Chem. Soc.*, 67, 150–152.
- Orr, R. L. (1953) High temperature heat contents of magnesium orthosilicate and ferrous orthosilicate. *J. Am. Chem. Soc.*, 75, 528–529.
- Plackett, R. L. (1960) *Principles of Regression Analysis*. Clarendon Press, London.
- Robie, R. A., P. M. Bethke and K. M. Beardsley (1967) Selected X-ray crystallographic data, molar volumes, and densities of minerals and related substances. *U. S. Geol. Surv. Bull.* 1248.
- and J. W. Stout (1963) Heat capacity from 12 to 305°K and entropy of talc and tremolite. *J. Phys. Chem.*, 67, 2252–2256.
- and D. R. Waldbaum (1968) Thermodynamic properties of minerals and related substances at 298.15°K (25°C) and one atmosphere (1.013 bars) pressure and at higher temperatures. *U. S. Geol. Surv. Bull.* 1259.
- Shaw, H. R. and D. R. Wones (1964) Fugacity coefficients for hydrogen gas between 0° and 1000°C for pressures to 3000 atmospheres. *Am. J. Sci.*, 262, 918–929.
- Skippen, G. B. (1971) Experimental data for reactions in siliceous marbles. *J. Geol.*, 79, 457–481.
- Southard, J. C. (1941) A modified calorimeter for high temperatures. The heat content of silica, wollastonite, and thorium dioxide above 25°. *J. Am. Chem. Soc.*, 63, 3142–3146.
- Streat, J. (1973) *Singular Value Decomposition of a Matrix*. Computing Centre, University of British Columbia, Vancouver, Canada.
- Stull, D. R. and H. Prophet (1971) *JANAF thermochemical tables*. National Bureau of Standards, Washington, D. C.
- Swanson, H. E., R. K. Fuyat and G. M. Ugrinic (1955) Standard X-ray diffraction powder patterns. *U. S. Natl. Bur. Standards, Circ.* 539, No. 4.
- , N. T. Gilfrich and M. I. Cook (1956) Standard X-ray diffraction powder patterns. *U. S. Natl. Bur. Standards, Circ.* 539, No. 6.
- Taylor, K. and L. S. Wells (1938) Studies of heat of solution of calcium and magnesium oxides and hydroxides. *J. Res. Natl.*

- Bur. Standards, Sect. A, 21, 133-149.*
- Thompson, J. B., Jr. (1967) Thermodynamic properties of simple solutions. In P. H. Abelson, Ed., *Researches in Geochemistry, II*, p. 340-361. Wiley, New York.
- Todd, S. S. (1949) Heat capacities at low temperatures and entropies of magnesium and calcium fluorides. *J. Am. Chem. Soc., 71, 4115-4116.*
- Tuttle, O. F. (1949) Two pressure vessels for silicate-water studies. *Geol. Soc. Am. Bull., 60, 1727-1729.*
- Van Valkenburg, A. (1955) Synthesis of a fluoro talc and attempted synthesis of fluoro chrysotile and fluoro anthophyllite. *J. Res. Natl. Bur. Standards, Sect. A, 55, 215-217.*
- (1961) Synthesis of the humites $n\text{Mg}_2\text{SiO}_4 \cdot \text{Mg}(\text{F},\text{OH})_2$. *J. Res. Natl. Bur. Standards, Sect. A, 65, 415-428.*
- Victor, A. C. and T. B. Douglas (1963) Thermodynamic properties of magnesium oxide and beryllium oxide from 298 to 1200°K. *J. Res. Natl. Bur. Standards, Sect. A, 67, 325-329.*

*Manuscript received, March 27, 1978;
accepted for publication, April 23, 1979.*